

Heart and Lung Sounds Dataset Recorded From a Clinical Manikin Using Digital Stethoscope (HLS-CMDS)

S. Chidharth, S. Divakar , V. Vijayan

Department of Electronics and Instrumentation Engineering,
St. Joseph's College of Engineering,
OMR, Chennai 600119, TN, India.

Abstract. Heart and lung sounds are crucial for healthcare monitoring. Recent improvements in stethoscope technology have made it possible to capture patient sounds with enhanced precision. In this dataset, we used a digital stethoscope to capture both heart and lung sounds, including individual and mixed recordings. To our knowledge, this is the first dataset to offer both separate and mixed cardiorespiratory sounds. The recordings were collected from a clinical manikin, a patient simulator designed to replicate human physiological conditions, generating clean heart and lung sounds at different body locations. This dataset includes both normal sounds and various abnormalities (i.e., murmur, atrial fibrillation, tachycardia, atrioventricular block, third and fourth heart sound, wheezing, rhonchi, pleural rub, fine crackle, and coarse crackle sounds). The dataset includes audio recordings of chest examinations performed at different anatomical locations, as determined by specialist nurses. Each recording has been enhanced using frequency filters to highlight specific sound types. This dataset is useful for applications in artificial intelligence, such as automated cardiopulmonary disease detection, sound classification, unsupervised separation techniques, and deep learning algorithms related to audio signal processing.

Keywords: digital stethoscope, cardiorespiratory sounds, heart sounds, lung sounds, mixed recordings, clinical manikin, patient simulator, abnormal heart sounds, murmur, atrial fibrillation, tachycardia, atrioventricular block, S3 and S4 heart sounds, wheezing, rhonchi, pleural rub, fine crackles, coarse crackles, chest auscultation, anatomical recording locations, frequency filtering, biomedical signal processing, audio signal enhancement, artificial intelligence in healthcare, automated disease detection, sound classification, unsupervised source separation, deep learning, medical audio dataset, cardiopulmonary diagnosis.

I. BACKGROUND

Cardiopulmonary diseases are significant contributors to global mortality rates. Chronic respiratory diseases, such as asthma, were responsible for over 147 000 deaths in 2022 alone [1]. Meanwhile, cardiovascular diseases remain the leading cause of death worldwide, accounting for approximately 18.6 million deaths

annually [2]. Therefore, it is crucial to accurately analyze both heart and lung functions.

Auscultation of heart sound (HS) and lung sound (LS) plays a vital role in diagnosing a variety of cardiopulmonary conditions [3]. Although these acoustic signals are weak, they hold essential medical information [4]. In 1816, Rene´ Laennec invented the first stethoscope to listen to body sounds, which has

evolved over the years from a simple acoustic device to more sophisticated digital versions [5].

Technological advancements have led to the development of electronic stethoscopes that convert sound waves into electrical signals, allowing for sound processing and recording [6], [7]. Digital stethoscopes are the latest generation of these auscultation devices. They not only have the features of electronic stethoscopes but also offer enhanced analysis capabilities, including integration with smartphones and cloud-based platforms for real-time analysis and sharing [8].

Artificial intelligence (AI) and machine learning algorithms have made significant improvements in real-time analysis and clinical decision-making [9], [10]. However, the effectiveness of these models heavily depends on the availability of high-quality datasets that contain diverse examples and enough dataset size. Such datasets are essential for training and validating AI models that perform sound classification, anomaly detection, and signal separation.

Currently, there are few available datasets containing HS and LS. The invention of patient simulators has become a critical point in clinical training and data collection, offering a risk-free and realistic environment for recording HS and LS. For example, the manikin used in this work is widely used for its realistic articulation and ability to simulate a broad range of clinical scenarios [11].

Several large-scale publicly available datasets have been developed to facilitate research in HS and LS analysis. The ICBHI 2017 dataset, introduced by Rocha et al., remains one of the most comprehensive LS datasets, including normal and pathological cases such as crackles and wheezes [12]. In 2019, Kun-Hsi Tsai et al. were the first to utilize a student auscultation manikin to record HS and LS at 8 kHz sampling rate. However, the dataset was focused only on specific lung conditions (i.e., normal, wheezing, rhonchi, and stridor) and normal heart sound (HS) only. Moreover, they

recorded HS and LS separately and mixed them later [13]. Compared to Kun-Hsi Tsai et al., we captured more diverse LS types, as well as heart abnormalities [13]. Later in 2021, Luay Fraiwan et al. recorded a dataset, focused solely on LSs [14]. Similarly, Jorge Oliveira et al. introduced the "CirCor DigiScope Phonocardiogram" dataset. They collected over 5000 HS recordings but lacked LS data [15]. In contrast to Fraiwan et al. [14] and Oliveira et al. [15], who focused solely on LSs and HSs, respectively, our dataset includes heart, lung, and mixed recordings. In 2022, Julio Alejandro Valdez et al. gathered a cardiopulmonary dataset which provided separate HS and LS files recorded simultaneously but did not offer mixed recordings [16]. Unlike this work, we recorded mixed sound recordings, which are particularly valuable for developing unsupervised algorithms like blind source separation, allowing for analysis of the natural overlap between HS and LS.

Compared to previous works, which used an electronic stethoscope, our work utilizes a digital stethoscope, providing improved recording quality, a higher sampling rate, and better resolution. Our dataset also offers better sound quality due to a combination of hardware-based noise reduction and post-recording software filtering. In addition, it covers a wider range of heart and lung abnormalities. A key advantage of using the manikin is its ability to provide clear, isolated recordings of heart-only, lung-only, as well as heart-lung mixture sounds recorded simultaneously in a risk-free and realistic environment.

This dataset is particularly valuable for developing machine-learning algorithms for detecting heart and lung diseases. It is ideal for biomedical engineering and AI researchers focused on disease detection, HS-LS classification, and signal processing related to audio data. This dataset can be useful for various signal processing algorithms, such as principal component analysis (PCA), independent component analysis (ICA), support vector machine (SVM), convolutional neural networks (CNNs), and filtering. The dataset is useful for both supervised and unsupervised learning methods. Distinct HS and LS are useful for supervised methods,

such as classification algorithms. For unsupervised methods, such as clustering and blind source separation, the mixture recordings offer a rich resource for exploring the separation of overlapping signals.

We utilized this dataset in signal processing and machine learning studies. In [17], we proposed a modified affine non-negative matrix factorization (NMF) method for blind separation of HS and LS. This method used a parallel structure of multilayer units and exploited the periodic nature of heart and lung signals, achieving better performance than existing methods. In [18], we introduced a novel framework integrating large language models (LLMs) with non-NMF for source separation. This study represents the first integration of LLMs with NMF, marking a novel advancement in the field. The approach demonstrated its potential to enhance medical sound analysis for disease diagnostics.

II. COLLECTION METHODS AND DESIGN

Setup and Environment

Fig. 1 shows the diagram of our data acquisition process. We performed auscultation in a controlled, quiet, and noise-free environment [Fig. 2(a)]. We positioned the patient simulator in a sitting position to simulate realistic conditions for LS and HS recordings [Fig. 2(b)].

We recorded sounds from various chest locations depending on whether we were capturing HS or LS (Fig. 3). For the mixed recordings, we selected the location from either heart or lung zones. We performed lung recordings from both the right and left sides of the chest, with each side divided into three zones: upper, middle, and lower. We recorded sounds from the anterior chest because the manikin has speakers only on the anterior side, making posterior auscultation impractical.

We used standard lung auscultation landmarks [19]: upper anterior (UA), which is on ribs 2–4; middle anterior (MA), located at the anterior surface of ribs 4–

6; and lower anterior (LA), placed over ribs 6–8, 45° down from nipple. For heart auscultation, we performed auscultation over the classic sites

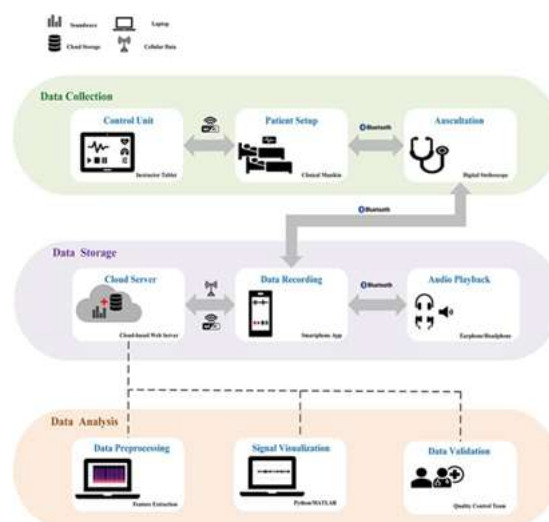


FIG. 1. Data acquisition system architecture and workflow. The process consists of three main steps: data collection, data storage, and data analysis. The data collection phase involves setting up the patient, controlling the recording process, and annotating the data. The collected signals are then transmitted and stored in a cloud server. Finally, the data analysis stage includes preprocessing, visualization, and validation to ensure quality and reliability.



(a) (b)

FIG. 2. Setup and environment: (a) recording unit at professional practice collaboratory (PPC); and (b) manikin in a sitting position alongside the recording setup.

of auscultation [18] as follows.

1. Apex (A): Mitral area.

2. Right upper sternal border (RUSB): Aortic area.
3. Left upper sternal border (LUSB): Pulmonary area.
4. Left lower sternal border (LLSB): Tricuspid area.
5. Right costal margin (RC).
6. Left costal margin (LC).

The manikin plays HS and LS through multiple anatomically positioned speakers. This setup ensures that sound

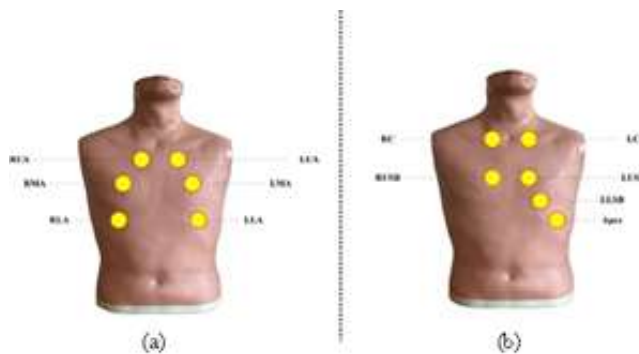


FIG. 3. Chest zone landmarks for recording: (a) LSs; and (b) HSs.

characteristics vary naturally across different locations, similar to human auscultation, due to distance, attenuation, and frequency response differences. Recording sounds from different locations is essential for AI model generalization. Labeling files by recording site is necessary to understand how auscultation position affects sound perception, enabling the development of spatially aware AI models for robust classification and source separation. For example, Fig. 4 shows four sample recordings from different locations with third HS (S3).

Clinical Skills Manikin and Control System

We utilized the CAE Juno™ nursing skills manikin, a mid-fidelity patient simulator designed to enhance clinical

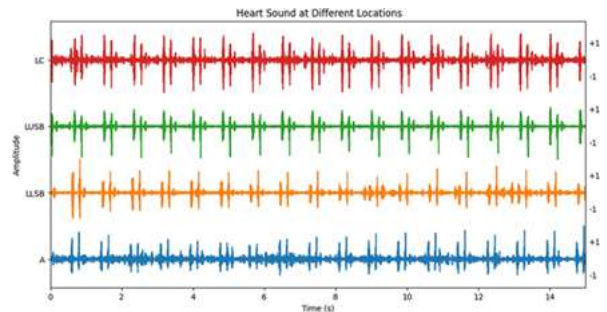


FIG. 4. Time-domain waveforms of four sample HS with third HS (S3) recorded from different locations. From top to bottom: Left costal margin (LC), left upper sternal border (LUSB), left lower sternal border (LLSB), and apex (A).



FIG. 5. Clinical manikin and the instructor tablet.

nursing skills. This manikin features interchangeable male and female chest skins, allowing gender switching to simulate male and female patients [21], [22]. We employed the CAE Maestro software, installed on a tablet, to control and monitor the manikin in real time. We connected the tablet to the manikin via a secure Wi-Fi connection, to remotely manage and customize a variety of patient sounds [23]. Fig. 5 shows the manikin and the tablet running the controlling software. The Manikin offers a range of pre-recorded HS and LS, which are synchronized with the cardiac cycle and ventilation of the left and right lungs, respectively [24]. The manikin plays pre-recorded HS and LS from real patients and does not artificially generate sounds.

Using the Maestro software, we adjusted the simulation parameters to suit the specific requirements of our

study, simulating real-life auscultation scenarios at various chest locations

For mixture recordings, we enabled both HS and LS and recorded them simultaneously. For each mixture, we also recorded the individual HS and LS separately without changing the stethoscope position. Since the clinical manikin plays pre-recorded sounds repeatedly, this method is equivalent to simultaneous recording. Therefore, our dataset provides a

reliable ground truth for source separation algorithms, as the mixed sounds are composed of the exact same heart and lung components captured individually.

The mixture recordings are suitable for evaluating source separation from single-channel recordings but not for multi-channel approaches such as PCA and ICA. For handling multi-channel approaches or studies that require only one sound type, we recorded additional pure HS and pure LS separately from different locations. Specifically, for single recordings, we first enabled only HSs and recorded them from standard auscultation landmarks, capturing various normal and abnormal HSs, including normal, late diastolic murmur, mid-systolic murmur, late systolic murmur, atrial fibrillation, S4 (fourth HS), early systolic murmur, S3 (third HS), tachycardia, and atrioventricular block. Next, we enabled only LSs and recorded the following types: normal, wheezing, fine crackle, rhonchi, pleural rub, and coarse crackle sounds. Each sound type was collected from different locations, and because the manikin's sounds are repeated, recording the same sound from multiple locations is equivalent to capturing it from multiple channels simultaneously.

The different cases in the dataset follow a uniform distribution of recording location, sound type, and gender, ensuring the dataset closely simulates real-world scenarios and covers all possible outcomes. We conducted a thorough screening of the mix.csv file to ensure that all possible combinations of the ten HS types and six LS types ($10 \times 6 = 60$ combinations) are included in the dataset.

Digital Stethoscope and Recording

We used the 3M™ Littmann® CORE Digital Stethoscope, 3M's most advanced model, to record LS and HS (Fig. 6). Each recording lasted 15 s, which was sufficient to capture at least one complete respiratory or cardiac cycle. The stethoscope has built-in frequency filters, allowing us to selectively capture HSs, LSs, or both, thereby enhancing precision



FIG. 6. Digital stethoscope and the recording app.

during the recording process. We applied three different filter modes based on the type of sound being captured: Bell mode for recording low-frequency HSs, Diaphragm mode for capturing high-frequency LSs, and Midrange mode for recording both HS and LS simultaneously. The amplification feature provided up to 40× sound enhancement, and the active noise cancellation effectively reduced ambient noise [25], [26]. One of the challenges in auscultation with digital stethoscopes is amplitude saturation, which can cause distortion and signal loss; to minimize this risk, we ensured proper stethoscope positioning and contact pressure during recording to avoid overloading the sensor.

We connected the stethoscope to the Eko software via Bluetooth, which enabled us to store the recordings directly on a mobile device. This mobile application pairs with the digital stethoscope, to record, visualize, and analyze cardiorespiratory sounds. It allows real-time monitoring, playback, and cloud-based storage of the recorded sounds. These recordings were subsequently uploaded to the cloud-based platform, making them accessible for download and further

analysis in .wav format on a personal computer (PC) or laptop.

Data Visualization

After transferring the recordings to a laptop, we visualized the time-domain signals that provide a clear view of the signal variations over time. We also generated time-frequency spectrograms to visualize the frequency content and signal energy over time. The resulting waveforms and spectrograms are essential for further analysis of the characteristics of the dataset and serve as a basis for future work in analyzing and interpreting the recorded data. Figs. 7 and 8 show three sample waveforms and spectrograms from the dataset, respectively. These spectrograms are included to demonstrate how the heart, lung, and mixed recordings appear in the time-frequency domain. They aim to convey the spectral patterns, overlap, and distinctions between different sound types, giving an intuitive insight into the structure of the dataset. While not part of the data processing itself, they help

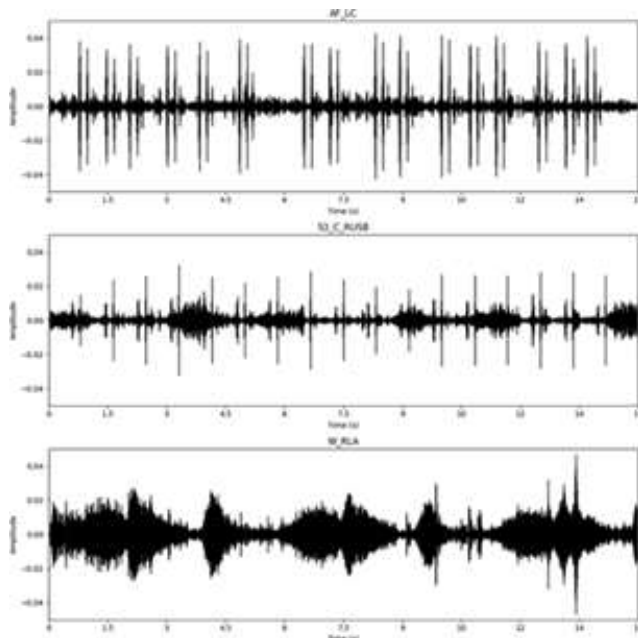


FIG. 7. Time-domain waveforms of three sample recordings. From top to bottom: HS with atrial fibrillation recorded from the left costal margin (AF LC), a mixture of HS and LS with third HS (S3) and crackles

recorded from the right upper sternal border (S3 C RUSB), and LS with wheezes recorded from the right lower anterior (W RLA).

validate that the dataset captures diverse acoustic features needed for signal processing applications.

Noise Handling

In real-world auscultation, chest sound recordings can be affected by various types of noise. These include ambient noise (background sounds from the environment, such as conversations, air conditioning, and equipment operation), stethoscope friction noise (caused by movement or improper contact between the stethoscope and the skin), and motion artifacts (unintended low-frequency fluctuations caused by patient movement or external disturbances). Additionally, biological noise from bodily functions such as muscle contractions and respiratory efforts can mask HS or LS.

Unlike human subjects, the manikin does not introduce biological noise or motion artifacts. To further minimize unwanted noise, recordings were conducted in a quiet, controlled environment, ensuring that external ambient noise was not introduced. The stethoscope was held steadily throughout the recording process to prevent motion artifacts and friction noise. Additionally, the digital stethoscope used in this study features built-in frequency-specific filters for heart, lung, and mixed sounds, effectively reducing irrelevant noise at the recording stage. In the preprocessing stage, we applied bandpass filtering to further refine the signals and remove any remaining unwanted frequency components.

III. VALIDATION AND QUALITY

The pre-recorded sounds are curated and provided by CAE Healthcare, originating from real patients, and synchronized with physiological parameters such as cardiac cycles and

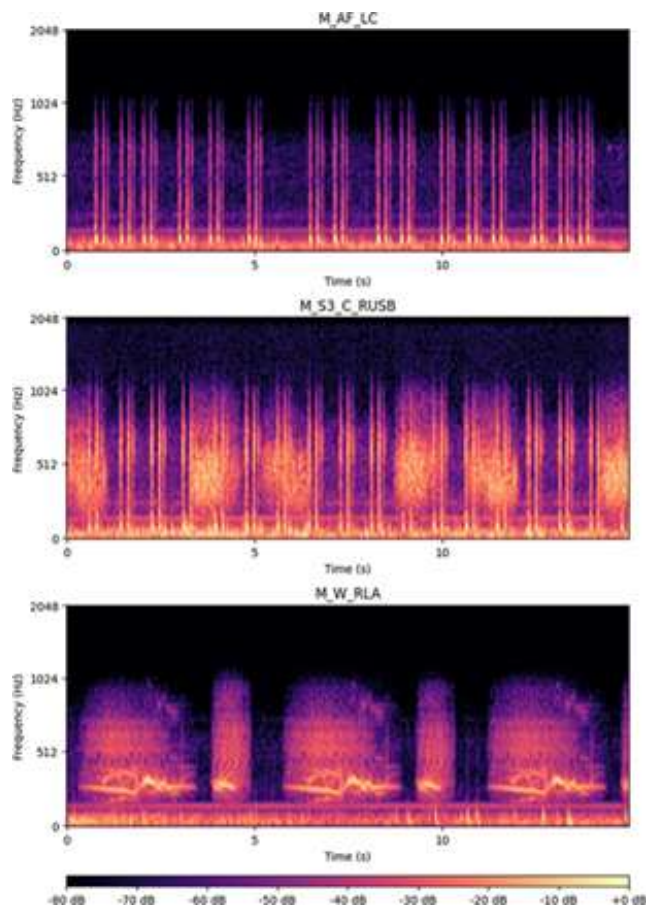


FIG. 8. Time-frequency spectrogram of three sample recordings. Spectrograms are two-dimensional representations of the audio signal in Fig. 5. x-axis represents time, while the y-axis represents frequency. The signal's energy is indicated by color. Black corresponds to areas of minimum energy, while yellow represents areas of maximum energy.

ventilation. These sounds undergo a quality assurance process by the manufacturer to ensure clinical accuracy and clarity. Additionally, we conducted post-recording validation by manually inspecting the waveforms to confirm the absence of signal artifacts. To ensure the accuracy and reliability of the collected data, we performed several validation measures across all stages of the data acquisition and processing. The nursing team assisted us in accurately identifying auscultation landmarks and ensured that clinical

aspects of the data collection process were properly followed. We made recordings in a controlled, noise-free environment with the manikin in a sitting position to eliminate external noise interference. Before recording the sounds, we precisely placed the stethoscope's diaphragm at standard auscultation points to minimize artifacts. After the recording session, we performed a qualitative analysis by listening to the audio files, ensuring they aligned with the expected patterns of HS and LS.

We selected a digital stethoscope with high amplification gain, active noise cancelation, and built-in frequency filters, which allowed us to capture sounds with minimal distortion. Technical specification of the stethoscope is given in Table I. Bluetooth data transmission ensures error-free transfer to a secure database without data loss or corruption [27], [28].

TABLE I. Technical Specification of the Digital Stethoscope

| Parameter | Value |
|-------------------------------------|---------------------------|
| Frequency Response (Bell Mode) | [20–200] Hz ^a |
| Frequency Response (Diaphragm Mode) | [100–500] Hz ^b |
| Frequency Response (Midrange Mode) | [50–500] Hz ^c |
| Amplification | Up to 40× |
| Recording Sample Rate | 22 050 Hz |
| Active Noise Cancelation | 85% ^d |

Note: dB = decibel; Hz = Hertz. aRapid decay @20 dB/octave above 300 Hz. bRapid decay @10 dB/octave below 200 Hz. cSmoothed response with peak @ 550 Hz (+20 dB). d@ [20–500] Hz, Reduction in ambient noise.

TABLE II. Clinical Manikin Technical Specifications

| Feature | Details |
|---------------------------|---------------------------------------|
| Dimensions | 162.56 × 52.07 × 25.4 cm ³ |
| Approximate Weight | 22.7 kg |
| Ambient Temperature Range | 4 to 40 °C |
| Battery System | 14.4 V Lithium-ion |
| Power Adapter | 100–240 V _{AC} , 50/60 Hz |
| Simulator Network | Wireless, IEEE 802.11 g |

Moreover, the selected manikin closely replicates real clinical scenarios and is approved by the U.S. National Council of State Boards of Nursing (NCSBN) [29], [30]. Additionally, the simulation lab team conducts regular maintenance and performs annual calibration to ensure the manikin’s sound system remains accurate over time. The reproducibility of the dataset is further supported by the standardized recording processes. Table II summarizes the manikin technical specifications.

IV. RECORDS AND STORAGE

The dataset consists of 535 audio recordings (268 Female, 267 Male) in .wav format, categorized into three primary groups: 50 HS recordings (HS.zip), 50 LS recordings (LS.zip), and 3 × 145 recordings of mixed HS and LS, as well as their heart and lung source sounds (Mix.zip). Each category is accompanied by a corresponding CSV file that provides metadata for the respective audio files. The CSV files (HS.csv, LS.csv, and Mix.csv) contain metadata about the corresponding audio files, including the file name, gender, HS, and LS type, and the anatomical location where we recorded the sound. The naming convention of the audio files of single recordings follows the structured format.

Gender Sound Type Location.wav

We denote the gender of the subject by F for female or M for male, followed by the sound type, and the

location on the chest where we recorded the sound. For the mixture dataset,

TABLE III. Sound Types

| Sound Type | | HS.zip | LS.zip | Mix.zip |
|--------------|-----|--------|--------|---------|
| Heart Sounds | NH | 9 | | 13 |
| | LDM | 6 | | 13 |
| | MSM | 7 | | 14 |
| | LSM | 5 | | 17 |
| | AF | 4 | | 15 |
| | S4 | 2 | | 16 |
| | ESM | 6 | | 13 |
| | S3 | 5 | | 15 |
| | T | 3 | | 16 |
| | AVB | 3 | | 13 |
| Lung Sounds | NL | | 12 | 28 |
| | W | | 7 | 28 |
| | FC | | 5 | 22 |
| | R | | 8 | 23 |
| | PR | | 9 | 25 |
| | CC | | 9 | 19 |

Note: NH = normal heart; LDM = late diastolic murmur; MSM = mid systolic murmur; LSM = late systolic murmur; AF = atrial fibrillation; S4 = fourth heart sound; ESM = early systolic murmur; S3 = third heart sound; T = tachycardia; AVB = atrioventricular block; NL = normal lung; W = wheezing; FC = fine crackle; R = rhonchi; PR = pleural rub; CC = coarse crackle.

TABLE IV. Chest Zones and the Number of Recordings

| Chest Zone | | No. in HS.zip | No. in LS.zip | No. in Mix.zip |
|------------------------------|------|---------------|---------------|----------------|
| Heart Auscultation Landmarks | RUSB | 7 | | 14 |
| | LUSB | 13 | | 13 |
| | LLSB | 10 | | 13 |
| | RC | 4 | | 13 |
| | LC | 6 | | 12 |
| | A | 10 | | 12 |
| Lung Auscultation Landmarks | RUA | | 7 | 12 |
| | LUA | | 11 | 12 |
| | RMA | | 5 | 12 |
| | LMA | | 9 | 11 |
| | RLA | | 10 | 9 |
| | LLA | | 8 | 12 |

we denote a sound ID from 0001 to 0145, added to H, L, or M for heart, lung, and mixed sound, respectively.

For example, M0002.wav is the second recorded sound, and H0002.wav and L0002.wav are its corresponding heart and lung source sounds. There are ten HS types and six LS types in the dataset. Table III shows the distribution of each sound type in the dataset. We recorded sounds from twelve distinct anatomical locations. Detailed demographic information of each recording location is described in Table IV.

V. INSIGHTS AND NOTES

This dataset is suitable for a wide range of research needs, including applications where the separation of HS and LS is crucial for analysis and advancing machine learning algorithms. However, there are some limitations to be aware of when using the dataset. While the simulated patient generates a wide range of pathological sounds, recorded from a controlled, low-noise environment, it may not fully replicate the complexity of real-world clinical environments. Clinical researchers should exercise caution when generalizing results from this dataset to real-world clinical settings without additional validation. For example, the dataset was recorded in a noise-free environment to ensure clean ground truth for algorithm validation. However, real-world clinical settings may include ambient noise. Although this dataset focuses on clarity, future work could explore adding noisy variants to support model robustness in practical applications. The users

of the dataset can add their own noise to the data to make a noisy version based on the type of noise they are interested in. Additionally, manikins lack real-world variability, patient-specific characteristics, and demographic diversity, which can affect the generalizability of machine learning models trained on such data. Moreover, over-reliance on simulator-generated recordings may lead to overfitting, as models trained exclusively on clean, structured sounds may struggle with real-world clinical auscultation, where patient movement, background noise, and anatomical differences play significant roles. Therefore, combining simulator-based datasets with real patient recordings in hybrid datasets can improve model robustness and

clinical applicability. In addition, HS and LS vary not only by gender but also by age [31]. We acknowledge the limitation of this study to adult subjects; however, pediatric manikins, such as the pediatric auscultation manikin (PAT) [32], are available for studies focusing on younger populations. Finally, this dataset lacks quantitative evaluations such as signal-to-noise ratio, annotation accuracy, and comparisons with real patient recordings. The manikin data is recorded from real patients and therefore there is a similarity between manikin-based and clinical data in terms of frequency content, temporal dynamics, and statistical distributions. However, previous studies have noted physiological correlations between HS and LS in real patients, but such natural coupling is not captured by the simulator and is not reflected in this dataset. Despite these limitations, simulated datasets play a complementary role in AI-based auscultation, particularly in transfer learning and pre-training AI models before fine-tuning on real-world data. A recent review by Pasterkamp and Melbye emphasizes the importance of maintaining a human-in-the-loop approach in AI-assisted auscultation, as current machine-learning models still face challenges in interpreting contextual and physiological factors [33]. Our dataset provides a structured foundation for training AI models while recognizing that real-world validation and hybrid dataset approaches remain essential for deployment in clinical practice. Additionally, the dataset is valuable for feature extraction in machine learning and acoustic signal processing algorithms, with potential applications in both education and clinical research. The stethoscope audio files can also be reused for training auscultatory skills among healthcare professionals and students. The dataset enriches the limited number of public datasets available for cardiopulmonary research and offers a reliable source of high-quality data for machine learning and signal processing tasks.

VI. SOURCE CODE AND SCRIPTS

The authors used Python Version 3.10 for data processing. The Python scripts are publicly available on

GitHub at the following repository: <https://github.com/Torabiy/HLS-CMDS>.

The authors used CAE Maestro software version 1.3 to control the patient simulators via an instructor tablet. The authors used Eko software version 5.11.1 (iOS) for storing the audio data from the stethoscope via a cellphone.

ACKNOWLEDGMENTS

Special thanks to the Mohawk Institute for Applied Health Sciences (IAHS) and Centre for Healthcare Simulation & Research (CHSR) for providing the simulators.

The authors used GPT-4 by OpenAI for text refinement, grammar, and spell-checking. No original research data were generated by AI, and all content was thoroughly reviewed by the authors.

Y.T.—main author, S.S.—supervision, and J.P.R.—co-supervision. The authors declared no conflicts of interest.

REFERENCES

- [1] Centers for Disease Control and Prevention, "Chronic respiratory diseases," CDC Wonder, Accessed: Sep. 13, 2024. [Online]. Available: <https://wonder.cdc.gov/controller/saved/D158/D389F360>
- [2] B. Baraeinejad et al., "Design and Implementation of an ultralow- power ECG Patch and smart cloud-based platform," *IEEE Trans. Instrum. Meas.*, vol. 71, pp. 1–11, 2022, Art. no. 2506811, doi: 10.1109/TIM.2022.3164151.
- [3] M. Sarkar, I. Madabhavi, N. Niranjana, and M. Dogra, "Auscultation of the respiratory system," *Ann. Thorac. Med.*, vol. 10, no. 3, pp. 158–168, Jul./Sep. 2015, doi: 10.4103/1817-1737.160831.
- [4] P. J. Bishop, "Evolution of the stethoscope," *J. R. Soc. Med.*, vol. 73, pp. 448–456, 1980, doi: 10.1177/014107688007300611.

- [5] J. P. Tourtier et al., "Auscultation in flight: Comparison of conventional and electronic stethoscopes," *Air Med. J.*, vol. 30, pp. 158–160, 2011, doi: 10.1016/j.amj.2010.11.009.
- [6] A. De Troyer, P. A. Kirkwood, and T. A. Wilson, "Respiratory action of the intercostal muscles," *Physiol. Rev.*, vol. 85, pp. 717–756, 2005.
- [7] Y. Torabi, S. Shirani, J. P. Reilly, and G. M. Gauvreau, "MEMS and ECM sensor technologies for cardiorespiratory sound monitoring—A comprehensive review," *Sensors (Basel, Switzerland)*, vol. 24, no. 21, p. 7036, 2024.
- [8] B. Baraeinejad et al., "Clinical IoT in practice: A novel design and implementation of a multi-functional digital stethoscope for remote health monitoring," Nov. 7, 2023, TechRxiv, doi: 10.36227/techrxiv.24459988.
- [9] B. Rahmatikaregar et al., "A review of automatic cardiac segmentation using deep learning and deformable models," in *Artificial Intelligence in Healthcare and Medicine*, 1st ed. Boca Raton, FL, USA: CRC Press, 2022, p. 29, doi: 10.1201/9781003120902.
- [10] B. Baraeinejad et al., "Design and implementation of an IoT-based respiratory motion sensor," 2024, arXiv:2412.05405.
- [11] "Enhancing nursing simulation education with CAE Juno: A leap forward in clinical skills training," WorldPoint. Accessed: Sep. 23, 2024. [Online]. Available: <https://www.worldpoint.com/mena/blog/enhancing-nursing-simulation-education-with-cae-juno-a-leap-forward-in-clinical-skills-training/>
- [12] B. M. Rocha et al., "A respiratory sound database for the development of automated classification," in *Precision Medicine Powered by pHHealth and Connected Health. ICBHI 2017. IFMBE Proceedings*, vol. 66, N. Maglaveras, I. Chouvarda, and P. de Carvalho, Eds., Singapore: Springer, 2018, doi: 10.1007/978-981-10-7419-6_6.
- [13] K.-H. Tsai et al., "Blind monaural source separation on heart and lung sounds based on periodic-coded deep autoencoder," *IEEE J. Biomed. Health Informat.*, vol. 24, no. 11, pp. 3203–3214, Nov. 2020, doi: 10.1109/JBHI.2020.3016831.

- [14] L. Fraiwan et al., "A dataset of lung sounds recorded from the chest wall using an electronic stethoscope," *Data Brief*, vol. 35, 2021, Art. no. 106913, doi: 10.1016/j.dib.2021.106000.
- [15] J. Oliveira et al., "The CirCor DigiScope phonocardiogram dataset," *PhysioNet*, 2022, doi: 10.13026/tshs-mw03.
- [16] J. A. Valdez and P. Mayorga, "Cardiopulmonary sounds database," *IEEE Dataport*, 2022, doi: 10.21227/8jzz-3x76.
- [17] Y. Torabi et al., "A new non-negative matrix factorization approach for blind source separation of cardiovascular and respiratory sound based on the periodicity of heart and lung function," 2023, arXiv:2305.01889.
- [18] Y. Torabi, S. Shirani, and J. P. Reilly, "Large language model-based nonnegative matrix factorization for cardiorespiratory sound separation," 2025, arXiv:2502.05757.
- [19] Physiopedia contributors, "Auscultation," *Physiopedia*. Accessed: Mar. 10, 2025. [Online]. Available: <https://www.physio-pedia.com/index.php?title=Auscultation&oldid=351421>
- [20] P. S. Rao, "Diagnosis of cardiac murmurs in children," *Vessel Plus*, vol. 6, 2022, Art. no. 22, doi: 10.20517/2574-1209.2021.105.
- [21] "Juno nursing skills manikin." Accessed: Sep. 23, 2024. [Online]. Available: <https://elevatehealth.net/solutions/brands/juno/>
- [22] "CAE Juno nursing skills manikin." *DiaMedical USA*. Accessed: Sep. 23, 2024. [Online]. Available: <https://www.diamedicalusa.com/CAE-Juno-Nursing-Skills-Manikin>
- [23] "CAE maestro user guide," *HeartSmart*. Accessed: Sep. 23, 2024. [Online]. Available: <https://www.heartsmart.com/pdf/cae-maestro-juno-user-guide-hs.pdf>
- [24] "Juno user guide," *Elevate Health*. Accessed: Sep. 23, 2024. [Online]. Available: https://elevatehealth.net/media/docs/905K600152_1_5_Juno_User_Guide.pdf
- [25] "3M™ Littmann® CORE Digital Stethoscope User Manual," *Gima*. Accessed: Sep. 23, 2024. [Online]. Available: <https://www.gimaitaly.com/DocumentiGIMA/Manuali/EN/M32600EN.pdf>
- [26] "3M™ Littmann® CORE Digital Stethoscope," *Littmann*. Accessed: Sep. 23, 2024. [Online]. Available: https://www.littmann.com/3M/en_US/littmann-stethoscopes/advantages/core-digital-stethoscope/
- [27] V. Oliynik, "On potential effectiveness of integration of 3M Littmann 3200 electronic stethoscopes into the third-party diagnostic systems with auscultation signal processing," in *Proc. IEEE 35th Int. Conf. Electron. Nanotechnol. (ELNANO)*, Kyiv, Ukraine, 2015, pp. 417–421, doi: 10.1109/ELNANO.2015.7146923.
- [28] A. Kaushik, "Towards the development of a breath-tracking mobile application," M.S. thesis, Dept. Comput. Sci., California State Univ., Northridge, CA, USA, 2020. [Online]. Available: <https://scholarworks.calstate.edu/downloads/7d278w841>
- [29] C. A. E. Healthcare, "CAE Healthcare introduces CAE Juno clinical skills manikin at INACSL nursing." Accessed: Sep. 23, 2024. [Online]. Available: <https://www.cae.com/news-events/press-releases/cae-healthcare-introduces-cae-juno-clinical-skills-manikin-at-inacsl-nursin/>
- [30] M. Alexander et al., "NCSBN simulation guidelines for prelicensure nursing programs," *J. Nursing Regulat.*, vol. 6, no. 3, pp. 39–42, 2015. [Online]. Available: https://www.ncsbn.org/public-files/JNR_Simulation_Supplement.pdf
- [31] V. Gross et al., "The relationship between normal lung sounds, age, and gender," *Am. J. Respir. Crit. Care Med.*, vol. 162, no. 3, pp. 905–909, 2000, doi: 10.1164/ajrccm.162.3.9905104.
- [32] Cardionics, "PAT Basic—Affordable pediatric auscultation manikin." Accessed: Mar. 10, 2025. [Online]. Available: <https://cardionics.com/en/product/pat-basic-affordable-pediatric-auscultation-manikin/>
- [33] H. Pasterkamp and H. Melbye, "Machines are learning chest auscultation. Will they also become our teachers?" *Chest Pulmonary*, vol. 2, no. 4, 2024, Art. no. 100079, doi: 10.1016/j.chpulm.2024.100079.